Probabilistic Fatigue Crack Initiation and Propagation Fields Using the Strain Energy Density

J. A. F. O. Correia,[a,1] P. J. Huffman,[b] A. M. P. De Jesus,[a] G. Lesiuk,[c] J. M. Castro,[a] R. A. B. Calcada,[a] and F. Berto[d]

[a] Faculty of Engineering, University of Porto, Porto, Portugal

[b] John Deere, One John Deere Place, Moline, IL, USA

[c] Laboratory of Materials Science and Engineering, University of Cantabria, Santander, Cantabria, Spain

[d] Department of Industrial and Mechanical Design, Norwegian University of Science and Technology, Trondheim, Norway

[1] jacorreia@inegi.up.pt

Построение вероятностных полей зарождения и роста усталостных трещин по критерию плотности энергии деформации

Ж. А. Ф. О. Коррейя[a], П. Дж. Хаффман[б], А. М. П. Де Хесус[a], Г. Лесюк[в], Ж. М. Кастро[a], Р. А. Б. Кальсада[a], Ф. Берто[г]

[a] Машиностроительный факультет, Университет Порту, Порту, Португалия

[б] Штаб-квартира Джон Дир, Молин, Иллинойс, США

[в] Лаборатория материаловедения и машиностроения, Кантабрийский университет, Сантандер, Кантабрия, Испания

[г] Факультет промышленного и инженерного проектирования, Норвежский университет естественных и технических наук, Тронхейм, Норвегия

Рост усталостной трещины достаточно хорошо изучен и описан с помощью нескольких моделей, наиболее известными из которых являются уравнения Париса. Хотя процессы инициирования и распространения усталостных трещин изучаются отдельно, ряд исследователей подробно рассматривают взаимосвязь между этими двумя усталостными процессами. В этом направлении предложено несколько моделей роста усталостных трещин, основанных на локальных подходах, в частности модель единого роста (UniGrow). Для некоторого элементарного объема материала процесс роста усталостной трещины можно представить в виде последовательности повторного зарождения (инициирования) трещины. В настоящее время Хаффман разработал концепцию плотности энергии деформации, основанную на циклической долговечности и развитии усталостной трещины по типу Волкера. Модель Хаффмана, базирующаяся на локальной плотности деформации, используется для прогнозирования инициирования и распространения усталостной трещины в стали P355NL1, применяемой в сосудах высокого давления. Данная модель сочетается с обобщенной вероятностной моделью усталости, ранее предложенной одним из соавторов, суть которой состоит в генерации вероятностных полей инициирования и распространения усталостных трещин. Получены локальные напряжения и деформации в вершине трещины, объединяющие их линейно-упругие и упругопластические составляющие. Для нескольких значений коэффициента асимметрии цикла напряжений R оценены вероятностные поля скоростей роста уста-

лостных трещин с учетом параметров повреждения, параметра Смита–Ватсона–Топпера (SWT) и эквивалентных параметров амплитуды напряжения. Сравнение экспериментальных данных по приращению усталостной трещины с прогнозируемыми вероятностными полями ее роста показывает их тесную корреляцию.

Ключевые слова: усталость, инициирование трещины, рост трещины, локальная энергия деформации, обобщенная вероятностная модель, результаты испытаний на выносливость.

Introduction. Fatigue crack growth (FCG) process is associated with the formation of new crack faces. Formation of new crack surfaces need the activation energy. During fatigue process, this energy can be delivered to the process zone due to work of external loading. The dissipated damage energy is responsible for "jump like" fatigue crack growth. This concept is reflected in several formulas and ideas of fatigue crack growth [1–8], where the fatigue crack growth process is treated as a discrete process where the local fatigue crack growth is associated with a specified "unit" of fatigue crack growth (see Fig. 1):

$$\frac{da}{dN} = \frac{d^*}{N_f}. \tag{1}$$

Generally, the fatigue crack growth can be postulated as a process involving the following assumptions [2, 4, 5, 7, 8]:

(i) the material is composed of simple particles of a finite dimension, ρ, which represents the elementary material block size, below which material cannot be regarded as a continuum (Fig. 1);

(ii) ahead crack tip exist two plastic zones; static and cyclic (Fig. 1);

(iii) the fatigue crack tip is supposed to be equivalent to a notch with radius, ρ;

(iv) the fatigue crack growth process is considered as representing successive crack increments (after N_f cycles) due to crack re-initiations over the distance, d^*, ρ.
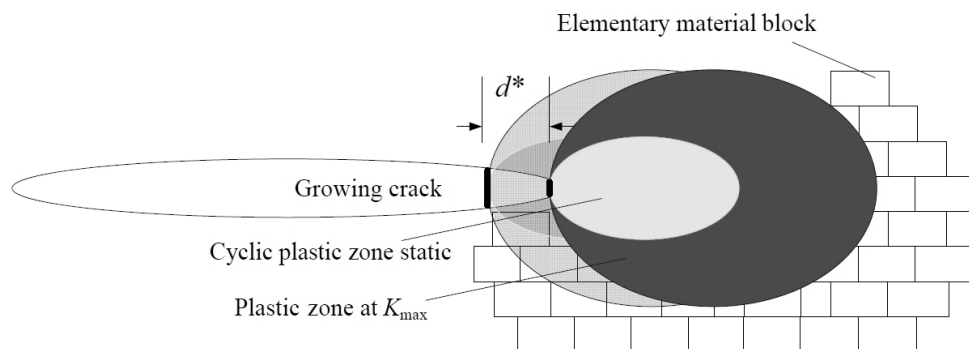

Fig. 1. Discrete nature of fatigue fracture process.

The mentioned assumptions are already reflected in several fatigue crack propagation models based on low-cycle fatigue (LCF) data [9–14].

Another relevant aspect in these local approaches is the calculation of local stresses and strains at the crack tip. The most commonly used local approaches are based on Coffin–Manson & Morrow relationships [15–17] with or without the influence of the mean stress effects. Glinka [2], Peeker and Niemi [18], Noroozi et al. [7, 8], Hurley and Evans [19], among others, used in their studies the strain fatigue damage parameter. More

recently, Correia et al. [20], Hafezi et al. [21], and De Jesus and Correia [22] have used the Smith–Watson–Topper (SWT) local damage parameter [23]. The equivalent stress amplitude damage parameter, σ_{ar}, has been used for the fatigue crack growth modelling based on local approaches by Correia and Huffman [12, 13].

In this paper, probabilistic fatigue crack initiation and propagation fields are presented based on strain energy approach proposed by Huffman [24] and considering the generalized probabilistic fatigue model suggested by Correia et al. [25]. The Huffman fatigue crack growth model based on strain energy density is analyzed considering several fatigue damage parameter such as strain, Smith–Watson–Topper (SWT), and equivalent stress amplitude. An analysis of results from the application of the fatigue crack growth model proposed by Huffman using the different damage parameters and experimental data is done. The generalized probabilistic fatigue model is used aiming at generating probabilistic FCG fields, for the fatigue damage parameters under consideration. In this analysis, experimental fatigue data of the P355NL1 steel from the low-cycle fatigue and fatigue crack growth tests are used [26–28].

1. **Huffman Fatigue Crack Initiation and Growth Model**. The fatigue crack growth relations are established with the linear elastic fracture mechanics (LEFM) to evaluate the stress distributions in a material. The variables such as the geometry and loading are considered to obtain the fatigue crack growth rates. Glinka [2] was pioneer to relate the local stress and strain at the crack tip, by relating the strain energy distribution with the LEFM approach, and the fatigue failure of the material ahead the crack tip. This so called local approach is used to generate the fatigue crack growth for several crack lengths and calculating the stress or strain lives at the crack tip. These stresses and strains are used to obtain the number of cycles to failure, N_f, leading to the crack growth extension, Δa.

Huffman [24] proposed a fatigue damage parameter, D, based on strain energy density concepts and calculated it from cyclic stress-strain properties as given by

$$\left(\frac{U_e}{U_d \rho_c}\right)\left(\frac{U_p^*}{U_d \rho_c}\right) = D = \frac{2N}{2N_f}, \qquad (2)$$

where U_e is the elastic strain energy density, U_p^* is the complementary plastic strain energy density, ρ_c is the critical dislocation density, and U_d is the strain energy density that can be estimated by

$$U_d = \left(\frac{E}{2(1+\nu)}\right) \cdot |\vec{b}|^2, \qquad (3)$$

where ν is the Poisson's ratio and $\vec{b}$ is the Burger's vector. The value of $|\vec{b}|$ is equal to $2.52 \cdot 10^{10}$ m for iron, steel or similar metals as can be found in [24]. Finding the strain energy density by integrating the Ramberg–Osgood stress-strain relationship, results the damage equation in terms of materials parameters:

$$\left(\frac{2}{U_d^2 \rho_c^2}\right)\left(\frac{n'}{1+n'}\right)\left(\frac{1}{K'}\right)(\sigma_{max}^2)(\sigma_a)^{\frac{1+n'}{n'}} = D = \frac{1}{2N_f}, \qquad (4)$$

where σ_{max} is the maximum stress and σ_a is the stress amplitude. This equation can be used to generate the stress–life, strain–life, and fatigue crack growth curves from cyclic stress-strain properties.

The strain-life or Morrow parameters can be equated based on Eq. (3) resulting:

$$\sigma'_f = E\left(\frac{2}{U_d^2\rho_c^2}\left(\frac{1}{K'}\right)^{1/n'}\left(\frac{n'}{1+n'}\right)E^{(1+2n')/n'}\right)^{\frac{-n'}{1+3n'}}, \tag{5}$$

$$b = \frac{-n'}{1+3n'}, \tag{6}$$

$$\varepsilon'_f = E\left(\frac{2(K')^3}{U_d^2\rho_c^2 E}\left(\frac{n'}{1+n'}\right)\right)^{\frac{-1}{1+3n'}}, \tag{7}$$

$$c = \frac{-1}{1+3n'}, \tag{8}$$

where σ'_f is the fatigue strength coefficient, E is the elastic modulus, K' and n' are the cyclic Ramberg–Osgood parameters [29], b is the fatigue strength exponent, ε'_f is the fatigue ductility coefficient, c is the fatigue ductility exponent, and the ρ_c parameter can be determined by fitting the resultant strain–life curve to low-cycle strain–life data by solving the Eq. (4):

$$\rho_c = \sqrt{\left(\frac{2(2N_f)}{U_d^2 EN}\right)\left(\frac{n'}{1+n'}\right)\left(\frac{1}{K'}\right)^{(1/n')}(\sigma_{\max}^2)(\sigma_a)^{\left(\frac{1+n'}{n'}\right)}}. \tag{9}$$

Acording to [24], this parameter has been found between $1\cdot10^{15} \le \rho_c \le 3\cdot10^{16}$ m^{-2}. The Huffman fatigue crack growth rates using the Δa calibrator can be given by

$$\left(\frac{\Delta a}{U_d^2\rho_c^2}\right)\left(\frac{n'}{1+n'}\right)\left(\frac{1}{K'}\right)(\sigma_{\max}^2)(\sigma_a)^{\left(\frac{1+n'}{n'}\right)} = \frac{\Delta a}{N_f - 0} \approx \frac{da}{dN}. \tag{10}$$

In Eq. (10), the stresses, σ_a and $\sigma_{\max}$, are the local stresses near the crack tip that can be related to the load, geometry and fatigue crack growth parameters as proposed by Noroozi et al. [7, 8]. The fatigue crack growth rate considering the driving force is given by the following expression:

$$\frac{da}{dN} = C(\Delta\kappa)^\gamma, \tag{11}$$

where γ is the fatigue crack growth rate exponent, $\Delta\kappa$ is the fatigue crack growth driving force, and C is the fatigue crack growth rate coefficient that is given by

$$C = \left(\frac{\Delta a}{U_d^2\rho_c^2}\right)\left(\frac{n'}{1+n'}\right)(K')^{\frac{2}{1+n'}}(E)^{-\left(\frac{4n'+2}{n'+1}\right)}\left(\frac{1}{2}\right)^{\frac{1}{n'}}\left(\frac{1}{2\pi x}\right)^{\frac{1+3n'}{1+n'}}. \tag{12}$$

The fatigue crack growth driving force can be calculated as

$$\Delta\kappa = K_{\max}^p(\Delta K)^{1-p}, \tag{13}$$

$$K_{\max} = K_{\max, applied} + K_r, \tag{14}$$

$$\Delta K = \Delta K_{applied} + K_r, \tag{15}$$

$$p = \frac{2n'}{1+3n'}, \tag{16}$$

$$\gamma = \frac{2+6n'}{1+n'} = \frac{-2}{b+c}, \tag{17}$$

where ΔK is the total stress intensity factor range, $\Delta K_{applied}$ is the applied stress intensity factor range, $K_{\max, applied}$ is the maximum applied stress intensity factor, and K_r is the residual stress intensity factor. The adjustment of the Huffman fatigue crack growth model to the experimental results is made using the values of Δa and x as calibrators.

Several authors such as Correia et al. [20, 26, 27], Hafezi et al. [21], and De Jesus and Correia [22] proposed the use of the finite element method to obtain the stresses and strains fields based on linear-elastic and elastoplastic analyses. These numerical analyses to calculate the stresses and strains ahead of the crack tip can be used for fitting the fatigue crack growth model proposed by Huffman [24] to the experimental FCG data.

2. **Probabilistic Fatigue Damage Fields**. The probabilistic fatigue damage fields can be obtained using the generalized probabilistic model for several fatigue damage parameters proposed by Correia et al. [25]. Originally, the probabilistic model was proposed by Castillo and Fernández-Canteli [30] for stress- and strain-based fatigue damage parameters using the Weibull or Gumbel distributions. These probabilistic distributions satisfy the statistical and physical requirements of the fatigue data. Correia et al. [25] proposed the generalization of the fatigue probabilistic model for several damage parameters, considering the similarity between the power relations used for the deterministic damage representation and the hyperbolic probabilistic fields proposed by Castillo and Fernández-Canteli [30]:

$$\psi = q(N_f), \tag{18}$$

$$\psi = \kappa(2N_f)^{\alpha} + \psi_0, \tag{19}$$

where ψ is a fatigue damage parameter, ψ_0 is the fatigue (endurance) limit, κ and α are material constants, q is the decreasing function of total fatigue life, and finally, $2N_f$ or N_f represent the reversals to failure and the number of cycles to failure, respectively.

The deterministic power-law model is shown in Fig. 2. Several fatigue damage parameters based on stress, strain or energy criteria, describing the same schematic representation of Fig. 2, can be used in Eqs. (18) and (19).

Thus, fatigue damage parameters such as strain amplitude, ε_a, walker-like strain, ε_w, Smith–Watson–Topper, *SWT*, as well as the equivalent stress amplitude, σ_{ar}, among others, can be described by the generalized fatigue damage parameter, ψ:

$$\psi = \varepsilon_a, \tag{20}$$

$$\psi = \varepsilon_w = \varepsilon_a \left(\frac{2}{1-R_\sigma} \right)^{1-\gamma_w}, \tag{21}$$

$$\psi = SWT = \sigma_{\max}\varepsilon_a, \tag{22}$$

$$\psi = \sigma_{ar} = (\sigma_{\max})^{1-\gamma_w}(\sigma_a)^{\gamma_w}, \tag{23}$$

where the Walker exponent is defined as

$$\gamma_w = \frac{1+n'}{1+3n'}. \tag{24}$$

According to [31], the main advantage of the γ_w parameter is to describe the material mean stress fatigue behavior sensitivity, where for the SWT-life model, this parameter is equal to 0.5.
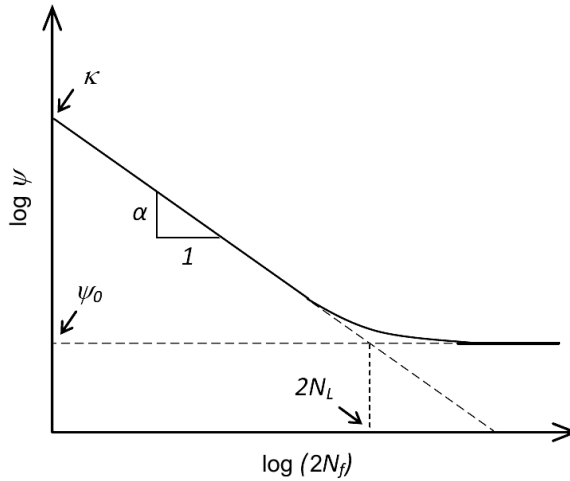

Fig. 2. Schematic representation of the deterministic power-law fatigue failure criterion [25].

In this way, the generalized probabilistic model to describe the fatigue failure criterion for several damage parameters was proposed by Correia et al. [25], based on Castillo and Fernández-Canteli probabilistic model [30], is given by

$$P = F(N_f^*; \sigma_{ar}^*) = 1 - \exp\left\{-\left[\frac{\log(N_f/N_0)\log(\psi/\psi_0) - \lambda}{\delta}\right]^{\beta}\right\}, \tag{25}$$

$$\log(N_f/N_0)\log(\psi/\psi_0) \geq \lambda, \tag{26}$$

where P is the probability of failure, N_0 and ψ_0 are values for normalizing, and β, δ, and λ are the dimensionless Weibull parameters. The normalizing parameters N_0 and ψ_0 are the threshold value for life and the corresponding value for the equivalent stress, respectively. The maximum likelihood method is used to estimate the Weibull parameters, where the details can be found in [30].

3. **Application of the Strain Energy Density Based Crack Propagation Model to Generate Probabilistic Fatigue Crack Initiation and Propagation Data**.

3.1. *Procedure to generate Probabilistic Fatigue Crack Initiation and Propagation Fields*. The procedure proposed to generate probabilistic fatigue crack initiation and propagation fields may be summarized in the following steps:

3.1.1. *Probabilistic Fatigue Crack Initiation Fields*:

(i) estimation of the Weibull parameters for the generalized probabilistic fatigue model based on strain, stress or energy damage parameters (Section 2), using experimental strain-life data from smooth specimens;

(ii) application of the Huffman fatigue crack initiation model to estimate the Morrow constants (Section 1);

(iii) computation of the probabilistic Huffman fatigue crack initiation models for several fatigue damage parameters.

3.1.2. *Probabilistic Fatigue Crack Propagation Fields*:

(i) the first step considered in probabilistic fatigue crack initiation fields (Section 2);

(ii) application of the Huffman fatigue crack propagation model based on strain energy density with probabilistic fatigue damage models (Section 1);

(iii) Computation of the $P - da/dN - \Delta K - R$ fields.

3.2. **Probabilistic Fatigue Crack Initiation Data**. The parameters of the cyclic elastoplastic stress–strain curves and elastic properties of the P355NL1 steel were collected in references [26–28]. These parameters were obtained based on experimental low-cycle fatigue tests of smooth specimens performed under strain controlled conditions carried out according the ASTM E606 standard. In Table 1 the cyclic stress-strain properties for the P355NL1 steel are shown.

T a b l e 1
Cyclic Stress-Strain Properties for P355NL1 Steel [26–28]

| Strain ratio R_ε	E, GPa	ν	K', MPa	n'
0			913.6	0.1459
-1	205.20	0.275	1022.3	0.1682
"-1" + "0"			948.35	0.1533

The Morrow constants obtained using the Coffin–Manson & Morrow relation [15–17] are presented in Table 2. In this table the Morrow constants estimates according to the assumption in the Huffman model [24] presented in Section 1 are also shown. This model allows evaluating the fatigue crack initiation phase based on strain energy. Equations (5)–(8) were used to estimate the Morrow constants and Eq. (9) used to obtain the critical dislocation density. A good agreement for the Morrow strain-life constants between the Huffman model and the Coffin–Manson & Morrow relation is verified (see Table 2). The critical dislocation density, ρ_c, estimated and presented in Table 2, is similar when compared with other materials of identical mechanical properties (see [24]).

T a b l e 2
Morrow Constants for P355NL1 Steel Calculated as per Eqs. (5)–(8)

| Strain ratio R_ε	Model	σ'_f, MPa	b	ε'_f	c	ρ_c, m/m^3
"-1" + "0"	Morrow equation	1005.5	-0.1033	0.3678	-0.5475	–
	Huffman model	959.0	-0.1050	1.08	-0.6850	$7.0 \cdot 10^{15}$

In Fig. 3, the stress–life, strain–life, and *SWT*–life curves are presented, being compared the experimental results with the Huffman fatigue crack initiation model predictions. In these figures, a good agreement between the experimental results and the fatigue crack initiation model predictions by Huffman [24] can be observed.
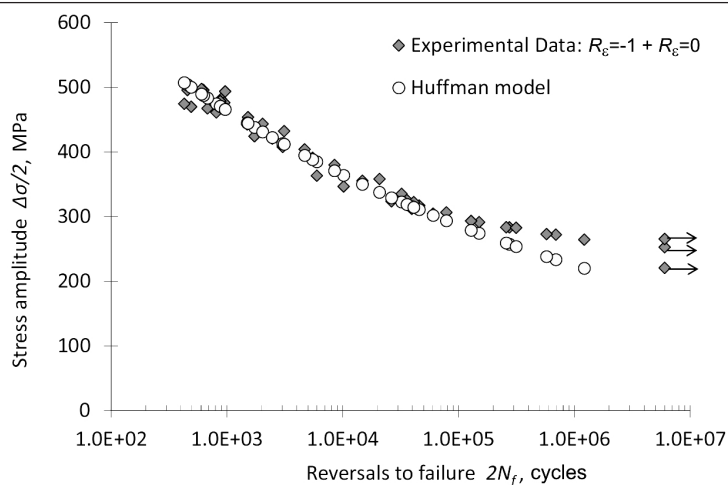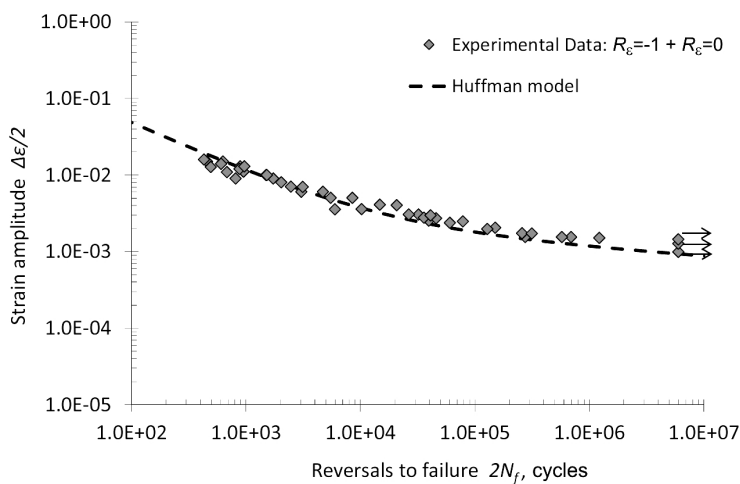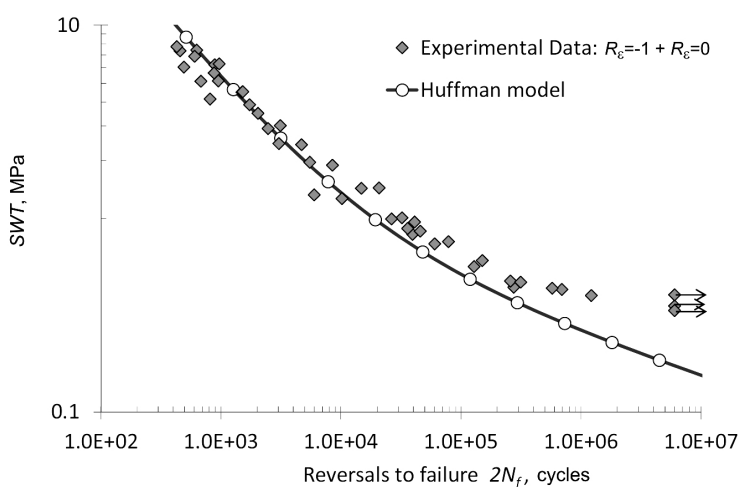
Fig. 3. Stress–life (a), strain–life (b), and *SWT*–life (c) curves of P355NL1 steel.

Figure 4 shows, respectively, the probabilistic fields for several fatigue damage parameters as strain amplitude, *SWT,* and equivalent stress amplitude, using the generalized probabilistic model [Eqs. (25) and (26)] presented in Section 2 and proposed by Correia et al. [25]. The Walker exponent for the P355NL1 steel is equal to 0.79 and was used to generate the probabilistic field (Fig. 4c). These probabilistic fields were used to generate the probabilistic Huffman fatigue crack growth fields.

3.3. ***Probabilistic Fatigue Crack Propagation Data****.* The fatigue crack propagation data of the P355NL1 steel collected in [26–28] were used to evaluate the fatigue crack growth model based on strain energy proposed by Huffman [24].

Fatigue crack growth (FCG) rates for several stress *R*-ratios under constant amplitude loading conditions were obtained using the ASTM E647 standard and considering the Paris law [32]. The CT specimens of P355NL1 steel were built with a width $W = 40$ mm and a thickness $B = 4.5$ mm. For the P355NL1 steel, the FCG tests were carried out for stress *R*-ratios, $R_\sigma = 0, 0.5,$ and 0.7. All FCG tests were carried out for stress *R*-ratios, $R_\sigma = 0,$ 0.5, and 0.7, in air at room temperature under a sinusoidal waveform at a maximum frequency of 20 Hz.

In this research, the results from the linear-elastic and elastoplastic finite element analyses ahead of the crack tip of the CT geometry are required and were generated by De Jesus and Correia [20, 22, 27]. In those analyses, the cyclic elastoplastic curve obtained experimentally was considered by De Jesus and Correia [20, 22, 27]. The residual stress intensity factor results, K_r, are presented in Fig. 5 against the applied stress intensity factor range, $\Delta K_{applied}$, for CT specimen built in P355NL1 steel, which were calculated by De Jesus and Correia [20, 22, 27]. The numerical model of the CT specimen was highly refined at the crack tip region in order to estimate the crack increment, Δa. De Jesus and Correia [20, 22, 26, 27] in their investigations estimated the Δa parameter as equal to $4.5 \cdot 10^{-3}$ m. This value was used in this research.

The fatigue crack growth model based on strain energy proposed by Huffman [24] with the generalized probabilistic model for several fatigue damage parameters was applied to CT specimen geometry made of P355NL1 steel. The fatigue crack growth rate constants for several fatigue damage parameters, such as, strain amplitude, SWT, and Walker stress amplitude, were obtained from Eqs. (10) and (11)–(17) are shown in Table 3.

The probabilistic Huffman fatigue crack growth rates based on strain, SWT, and Walker stress amplitude fatigue damage parameters for the P355NL1 pressure vessel steel taking into account several stress *R*-ratios, are shown in Figs. 6–8. Figure 9 shows that the models appear to be more sensitive to stress ratio effects compared to the measured fatigue crack growth rates. It can be seen that models which demonstrate high levels of stress ratio sensitivity show particularly poor correlation at high stress *R*-ratios, R_σ, for materials which seem insensitive to stress *R*-ratio effects. When compared to the stress-life or strain-life, however, these models don't demonstrate to be so inaccurate. Although the P355NL1 steel was tested at 2 strain *R*-ratios, R_ε, the stress *R*-ratios, R_σ, were not drastically different. Because of this, differences in the stress-strain behavior of the material at different stress *R*-ratios may not have been observed even if they exist. If the material demonstrates stress ratio-sensitive stress-strain behavior, it could make a difference in how the residual stress would be calculated at a crack tip. A difference in the behavior of the residual stress would influence the residual stress intensity factor, K_r, and therefore would influence the calculated stress ratio dependent fatigue crack growth rates. This would appear as a lack of stress-ratio effect in a material, when it could in actuality be the same stress ratio effect as far as what the material itself goes through at the crack tip, but it would be disguised by a change in cyclic stress-strain behavior influencing the residual stress profile differently at different stress-ratios.
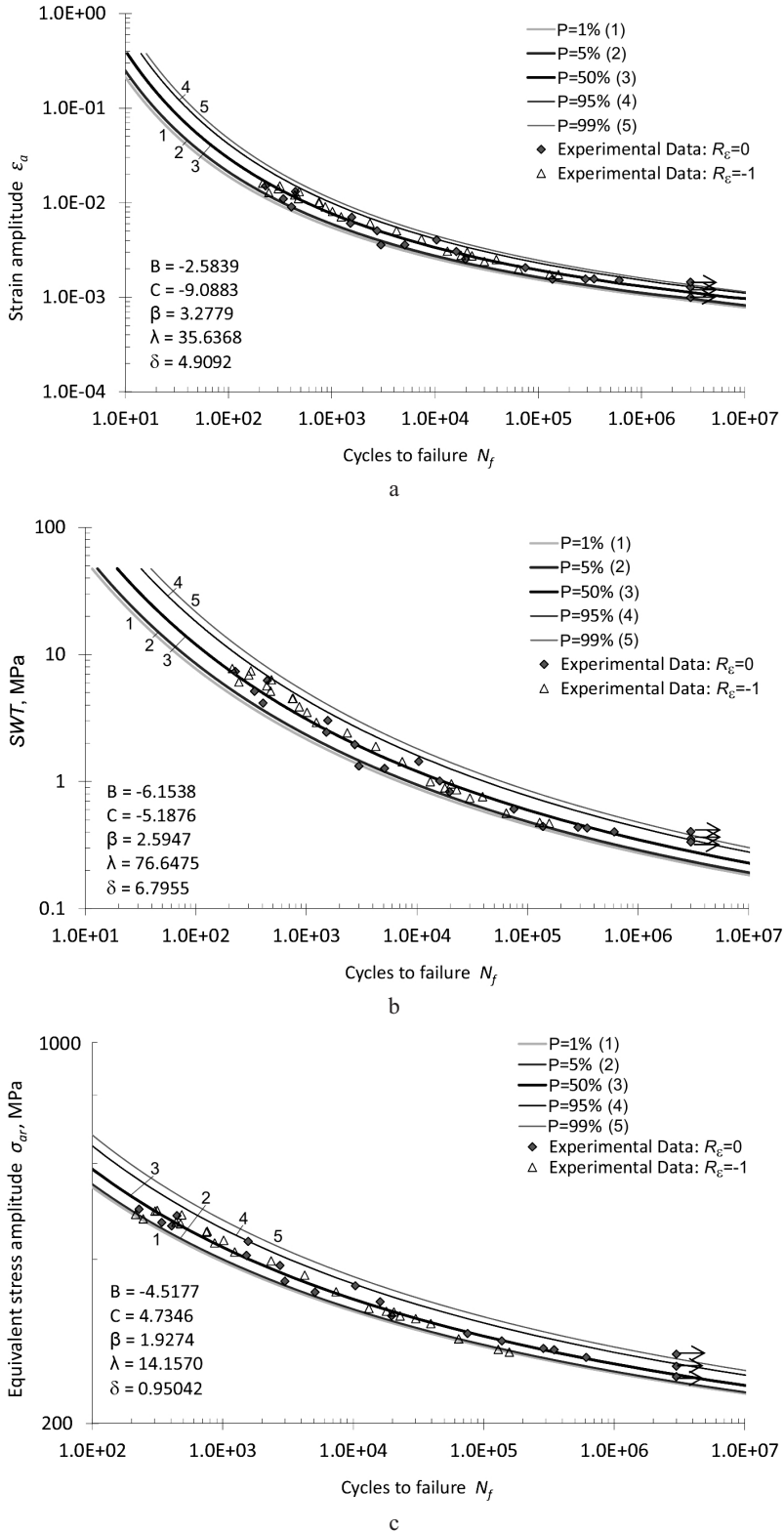
Fig. 4. Probabilistic $\varepsilon_a - N_f$ (a), $SWT - N_f$ (b), and $\sigma_{ar} - N_f$ (c) fields of P355NL1 steel.

T a b l e 3

Fatigue Crack Growth Rate Constants from Eqs. (10)–(17) for P355NL1 Steel

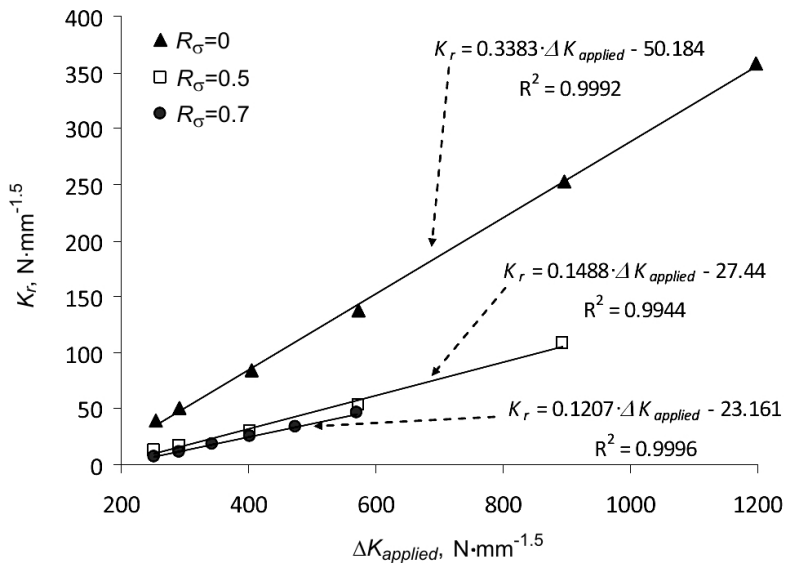| Fatigue damage parameter	Stress ratio R_σ	Δa, m	x, m	C, $\text{MPa}^\gamma \cdot \text{m}^{\gamma/2-1}$	γ	p
Strain amplitude ε_a	0	$4.5 \cdot 10^{-3}$	$0.7 \cdot 10^{-5}$	$8.488 \cdot 10^{-11}$	2.606	0.210
	0.5			$7.927 \cdot 10^{-11}$	2.627	0.210
	0.7			$7.004 \cdot 10^{-11}$	2.665	0.210
SWT	0	$4.5 \cdot 10^{-3}$	$3.0 \cdot 10^{-5}$	$2.872 \cdot 10^{-10}$	2.571	0.210
	0.5			$2.774 \cdot 10^{-10}$	2.582	0.210
	0.7			$2.598 \cdot 10^{-10}$	2.602	0.210
Walker stress amplitude σ_{ar}	0	$4.5 \cdot 10^{-3}$	$2.5 \cdot 10^{-5}$	$1.609 \cdot 10^{-11}$	2.611	0.210
	0.5			$1.495 \cdot 10^{-11}$	2.631	0.210
	0.7			$1.288 \cdot 10^{-11}$	2.685	0.210

Fig. 5. Residual stress intensity factor K_r as a function of the $\Delta K_{applied}$ for the CT geometry made in P355NL1 steel.

It is interesting to note that the strain amplitude probability field appears to be less sensitive to stress ratio. This could be evidence in support of using strain-life based calculations preferentially over stress-life based calculations under certain circumstances, though much further investigation would be necessary to determine that. These results are also evidence that care should be taken when selecting a mean stress effect, as overly sensitive models can lead to over-designed structures or under-designed structures depending on the expected load cases.
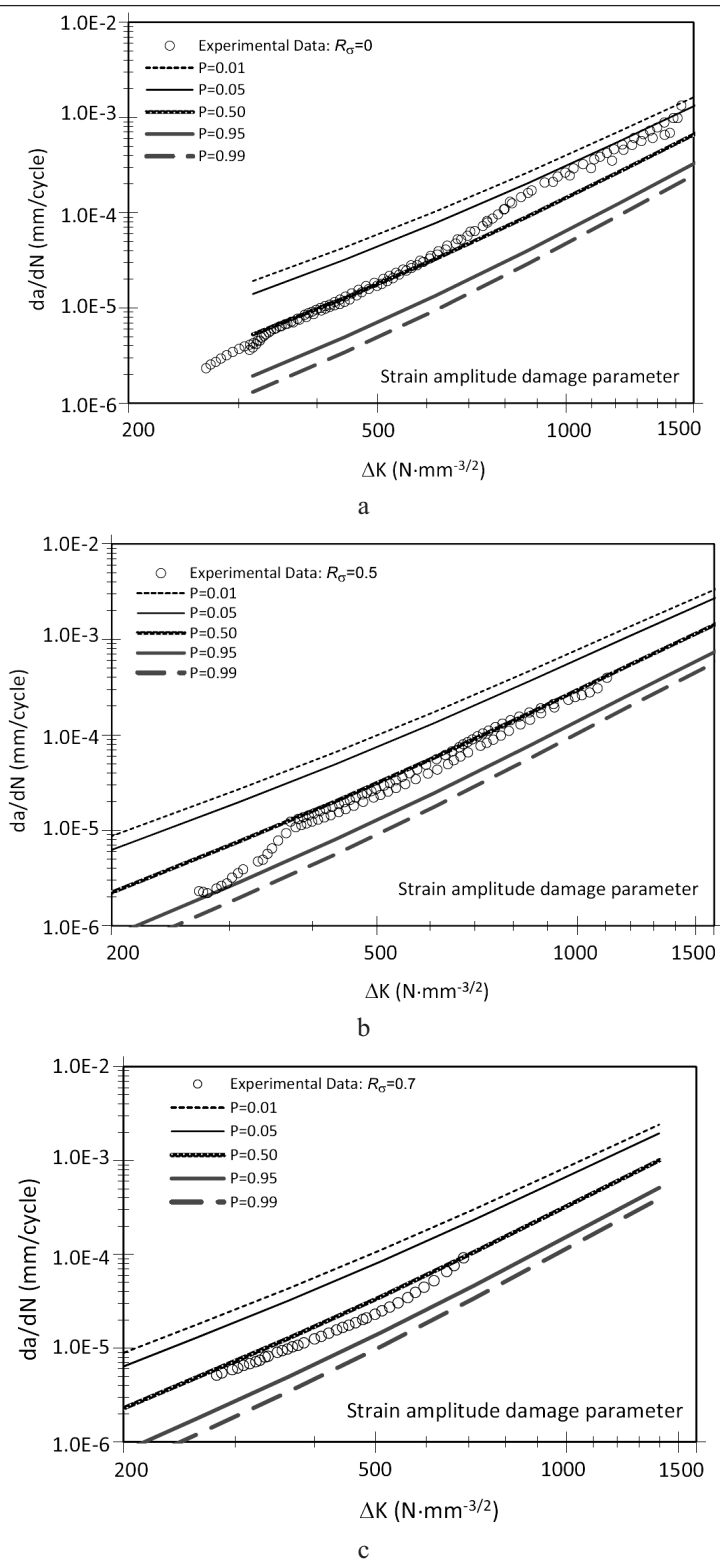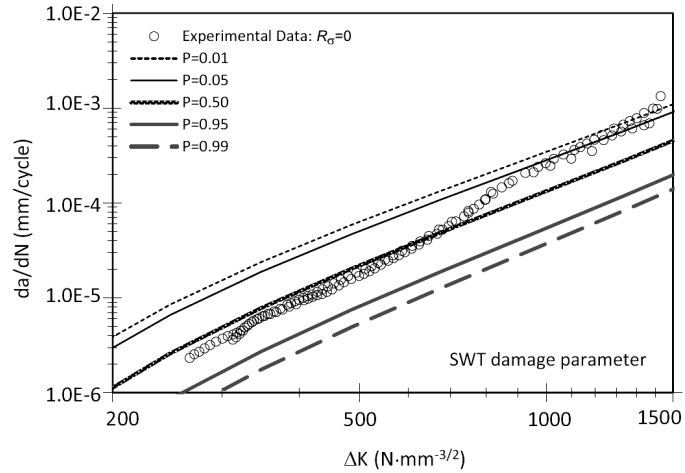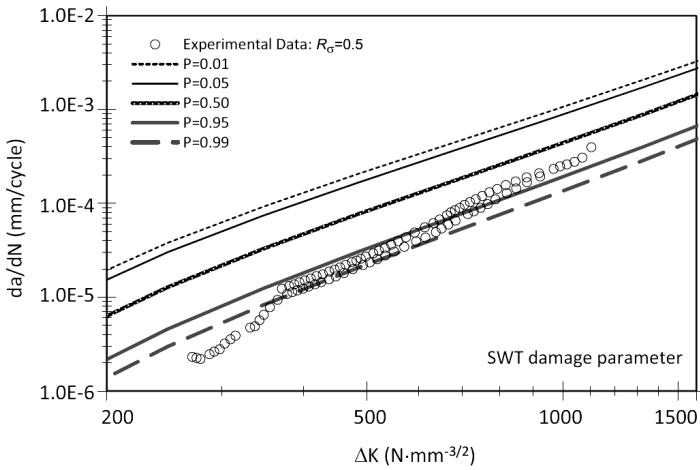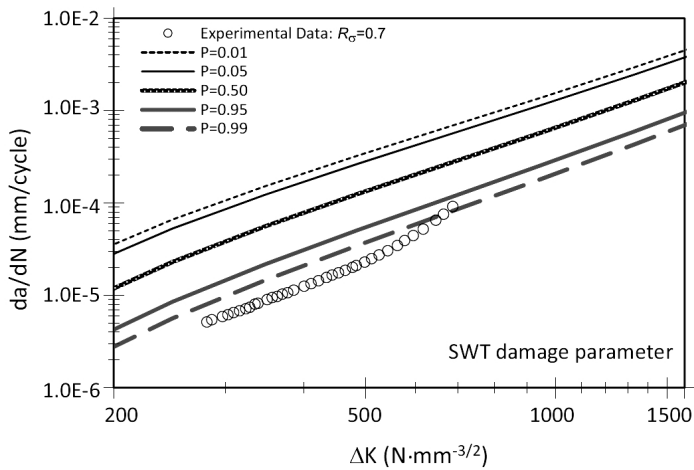
Fig. 6. Probabilistic prediction of the fatigue crack growth for P355NL1 steel based on Huffman FCG model and $P - \varepsilon_a - N$ field for $R_\sigma = 0$ (a), 0.5 (b), and 0.7 (c).

Fig. 7. Probabilistic prediction of the fatigue crack growth for P355NL1 steel based on Huffman FCG model and $P - SWT - N$ field for $R_\sigma = 0$ (a), 0.5 (b), and 0.7 (c).
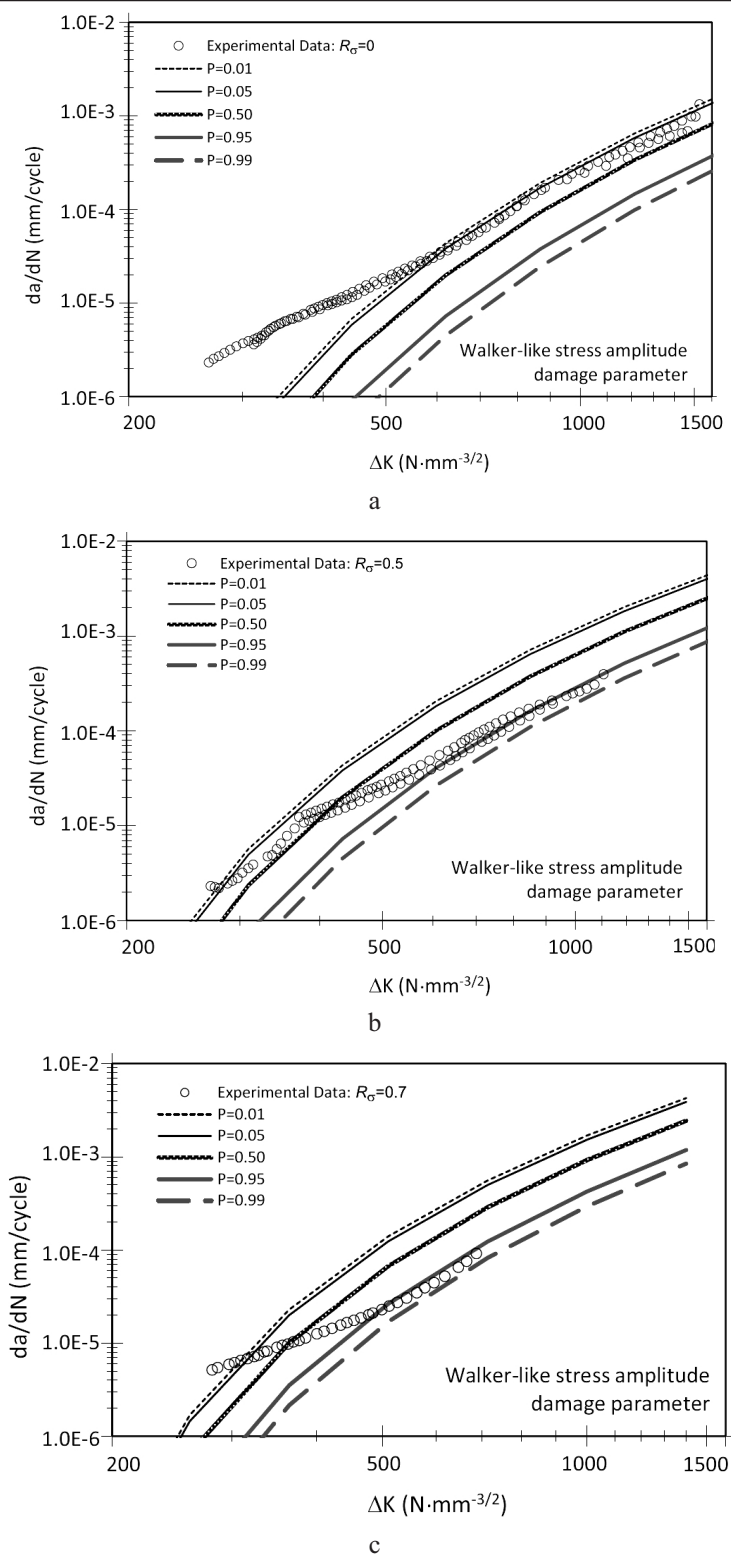
Fig. 8. Probabilistic prediction of the fatigue crack growth for P355NL1 steel based on Huffman FCG model and $P - \sigma_{ar} - N$ field for $R_\sigma = 0$ (a), 0.5 (b), and 0.7 (c).
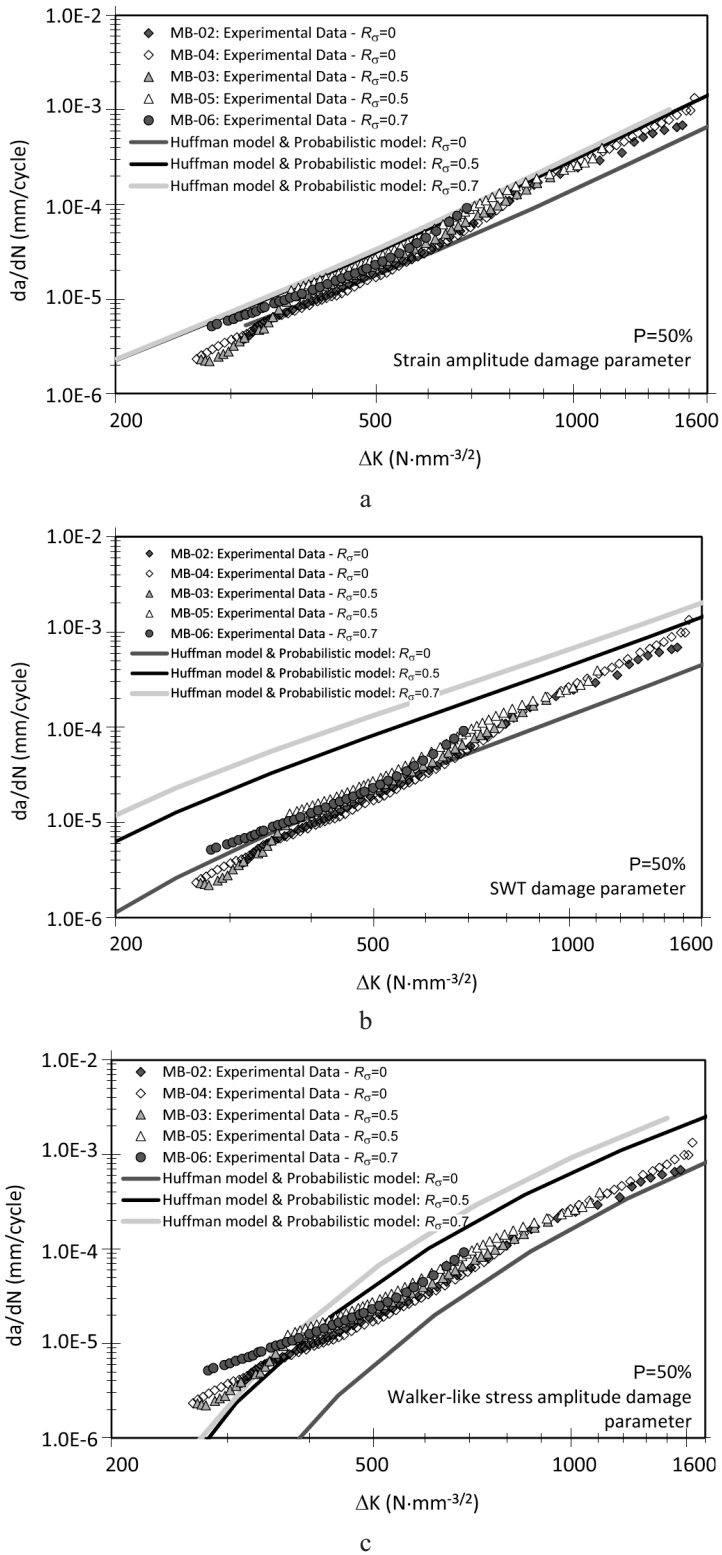
a

b

c

Fig. 9. Fatigue crack growth rates for the probability of failure equal to 50% based on Huffman model and $P - \varepsilon_a - N$ (a), $P - SWT - N$ (b), and $P - \sigma_{ar} - N$ (c) fields for several stress R-ratios.

C o n c l u s i o n s

1. The strain energy based fatigue crack initiation model proposed by Huffman can be used to estimate the Morrow constants giving good results when compared with experimental results.

2. The fatigue crack propagation model based on strain energy density proposed by Huffman can be used with results from the linear-elastic and elastoplastic numerical analyses and a good agreement is observed.

3. The Huffman model uses the calibration parameters, Δa and x, which are required for the fit of the Huffman FCG model to the experimental FCG data.

4. The combination of the Huffman fatigue crack growth model with the generalized probabilistic model allowed to generate the probabilistic fields for the fatigue crack propagation rates.

5. The probabilistic crack propagation fields generated using several fatigue damage parameters such as strain, SWT, and equivalent stress amplitude, allowed to conclude that the strain damage parameter is the most suitable for the P355NL1 steel, taking into account the comparison that is made with the experimental crack propagation data, showing that this material is not sensitive to the mean stress effects.

Р е з ю м е

Ріст тріщини від утомленості достатньо добре вивчено й описано за допомогою декількох моделей, найбільш відомими серед яких є рівняння Паріса. Хоча процеси ініціювання і поширення тріщин від утомленості вивчаються окремо, деякі дослідники детально розглядають взаємозв'язок між цими двома утомними процесами. У цьому напрямку запропоновано декілька моделей росту тріщин від утомленості, що базуються на локальних підходах, зокрема модель єдиного росту (UniGrow). Для деякого елементарного об'єму матеріалу процес росту тріщини від утомленості можна представити у вигляді послідовності повторного зародження (ініціювання) тріщини. На сьогодні Хаффман розробив концепцію густини енергії деформації на основі циклічної довговічності і поширення тріщини від утомленості по типу Волкера. Модель Хаффмана, що базується на локальній густині енергії деформації, використовується для прогнозування ініціювання і поширення тріщини від утомленості в сталі P355NL1, яка використовується для виготовлення посудин високого тиску. Дана модель поєднується з узагальненою імовірнісною моделлю утоми, раніше запропонованою одним із співавторів, суть якої полягає в генерації імовірнісних полів ініціювання і поширення тріщини від утомленості. Отримано локальні напруження і деформації у вершині тріщини, що об'єднують їх лінійно-пружні і пружнопластичні складові. Для декількох значень коефіцієнта асиметрії циклу напружень R оцінено імовірнісні поля швидкостей росту тріщин від утомленості з урахуванням параметрів пошкодження, параметра Сміта–Ватсона–Топпера (SWT) й еквівалентних параметрів амплітуди напруження. Порівняння експериментальних даних щодо приросту тріщини від утомленості з прогнозованими імовірнісними полями її росту свідчить про їх тісну кореляцію.

1. K. N. Raju, "An energy balance criterion for crack growth under fatigue loading from considerations of energy of plastic deformation," *Int. J. Fract. Mech.*, **8**, No. 1, 1–14 (1972).

2. G. Glinka, "A notch stress-strain analysis approach to fatigue crack growth," *Eng. Fract. Mech.*, **21**, No. 2, 245–261 (1985).

3. O. E. Andreikiv and M. V. Lishchyns'ka, "Equations of growth of fatigue cracks in inhomogeneous plates," *Mater. Sci.*, **35**, No. 3, 355–362 (1999).

4. M. Szata, *Modeling of Fatigue Crack Growth Using Energy Method* [in Polish], Publishing House of Wroclaw University of Technology, Wroclaw, Poland (2002).

5. M. Szata and G. Lesiuk, "Algorithms for the estimation of fatigue crack growth using energy method," *Arch. Civ. Mech. Eng.*, **9**, No. 1, 119–134 (2009).

6. N. W. Klingbeil, "A total dissipated energy theory of fatigue crack growth in ductile solids," *Int. J. Fatigue*, **25**, No. 2, 117–128 (2003).

7. A. H. Noroozi, G. Glinka, and S. Lambert, "A two parameter driving force for fatigue crack growth analysis," *Int. J. Fatigue*, **27**, Nos. 10–12, 1277–1296 (2005).

8. A. H. Noroozi, G. Glinka, and S. Lambert, "A study of the stress ratio effects on fatigue crack growth using the unified two-parameter fatigue crack growth driving force," *Int. J. Fatigue*, **29**, Nos. 9–11, 1616–1633 (2007).

9. L. Chen, L. Cai, and D. Yao, "A new method to predict fatigue crack growth rate of materials based on average cyclic plasticity strain damage accumulation," *Chinese J. Aeronaut.*, **26**, No. 1, 130–135 (2013).

10. A. S. F. Alves, L. M. C. M. V. Sampayo, J. A. F. O. Correia, et al., "Fatigue life prediction based on crack growth analysis using an equivalent initial flaw size model: application to a notched geometry," *Procedia Engineer.*, **114**, 730–737 (2015).

11. J. A. F. O. Correia, S. Blasón, A. M. P. De Jesus, et al., "Fatigue life prediction based on an equivalent initial flaw size approach and a new normalized fatigue crack growth model," *Eng. Fail. Anal.*, **69**, 15–28 (2016).

12. J. A. F. O. Correia, P. J. Huffman, A. M. P. De Jesus, et al., "Unified two-stage fatigue methodology based on a probabilistic damage model applied to structural details," *Theor. Appl. Fract. Mech.*, **92**, 252–265 (2017).

13. P. J. Huffman, J. Ferreira, J. A. F. O. Correia, et al., "Fatigue crack propagation prediction of a pressure vessel mild steel based on a strain energy density model," *Frattura ed Integrità Strutturale*, **11**, No. 42, 74–84 (2017), DOI: 10.3221/IGF-ESIS.42.09.

14. J. A. F. O. Correia, A. M. P. De Jesus, A. S. Ribeiro, and A. A. Fernandes, "Strain-based approach for fatigue crack propagation simulation of the 6061-T651 aluminium alloy," *Int. J. Mater. Struct. Integr.*, **11**, Nos. 1–3, 1–15 (2017), DOI: 10.1504/IJMSI.2017.087336.

15. L. F. Coffin, Jr., "A study of the effects of cyclic thermal stresses on a ductile metal," *Trans. ASME*, **76**, 931–950 (1954).

16. S. S. Manson, *Behavior of Materials under Conditions of Thermal Stress*, NACA TN-2933, National Advisory Committee for Aeronautics (1954).

17. J. D. Morrow, "Cyclic plastic strain energy and fatigue of metals," in: *Internal Friction, Damping, and Cyclic Plasticity*, ASTM STP 378, Philadelphia, PA (1965), pp. 45–87.

18. E. Peeker and E. Niemi, "Fatigue crack propagation model based on a local strain approach," *J. Constr. Steel Res.*, **49**, No. 2, 139–155 (1999).

19. P. J. Hurley and W. J. Evans, "A methodology for predicting fatigue crack propagation rates in titanium based on damage accumulation," *Scripta Mater.*, **56**, No. 8, 681–684 (2007).

20. J. A. F. O. Correia, A. M. P. De Jesus, A. Fernández-Canteli, "A procedure to derive probabilistic fatigue crack propagation data," *Int. J. Struct. Integr.*, **3**, No. 2, 158–183 (2012), DOI: 10.1108/17579861211235183.

21. M. H. Hafezi, N. N. Abdullah, J. A. F. O. Correia, and A. M. P. De Jesus, "An assessment of a strain-life approach for fatigue crack growth," *Int. J. Struct. Integr.*, **3**, No. 4, 344–376 (2012), DOI: 10.1108/17579861211281173.

22. A. M. P. De Jesus and J. A. F. O. Correia, "Critical assessment of a local strain-based fatigue crack growth model using experimental data available for the P355NL1 steel," *J. Press. Vess. Technol.*, **135**, No. 1, 011404-1–0114041-9 (2013).

23. K. N. Smith, P. Watson, and T. H. Topper, "A stress-strain function for the fatigue of metals," *J. Mater.*, **5**, No. 4, 767–778 (1970).

24. P. J. Huffman, "A strain energy based damage model for fatigue crack initiation and growth," *Int. J. Fatigue*, **88**, 197–204 (2016).

25. J. Correia, N. Apetre, A. Arcari, et al., "Generalized probabilistic model allowing for various fatigue damage variables," *Int. J. Fatigue*, **100**, Part 1, 187–194 (2017).

26. J. A. F. O. Correia, *An Integral Probabilistic Approach for Fatigue Lifetime Prediction of Mechanical and Structural Components*, Ph.D. Thesis, University of Porto (2014).

27. J. A. F. O. Correia, A. M. P. De Jesus, and A. Fernández-Canteli, "Local unified probabilistic model for fatigue crack initiation and propagation: application to a notched geometry," *Eng. Struct.*, **52**, 394–497 (2013).

28. J. A. F. O. Correia, A. M. P. De Jesus, P. M. G. P. Moreira, and P. J. Tavares, "Crack closure effects on fatigue crack propagation rates: application of a proposed theoretical model," *Adv. Mater. Sci. Eng.*, **2016**, 3026745 (2016), DOI: 10.1155/2016/3026745.

29. W. Ramberg and W. R. Osgood, *Description of the Stress–Strain Curves by the Three Parameters*, NACA TN-902, National Advisory Committee for Aeronautics (1943).

30. E. Castillo and Fernández-Canteli, *A Unified Statistical Methodology for Modeling Fatigue Damage*, Springer (2009).

31. N. E. Dowling, "Mean stress effects in strain-life fatigue," *Fatigue Fract. Eng. Mater. Struct.*, **32**, No. 12, 1004–1019 (2009).

32. P. C. Paris, M. P. Gomez, and W. E. Anderson, "A rational analytic theory of fatigue," Trend Eng., 13, 9–14 (1961).